ISSN 2079-1704. Хімія, фізика та технологія поверхні. 2023. Т. 14. № 1. С. 83-92

PACS: 78.66.Hf, 73.61.Ga doi: 10.15407/hftp14.01.083

**V.A. Karpyna [1], L.A. Myroniuk [1], D.V. Myroniuk [1], M.E. Bugaiova [1], L.I. Petrosian [1], O.I. Bykov [1], O.I. Olifan [1], V.V. Strelchuk [2], O.F. Kolomys [2], V.R. Romanyuk [2], K.S. Naumenko [3], L.O. Artiukh [3], O.Y. Povnitsa [3], S.D. Zahorodnia [3], A.I. Ievtushenko [1]**

# PHOTOCATALYSIS AND OPTICAL PROPERTIES OF ZnO NANOSTRUCTURES GROWN BY MOCVD ON Si, Au/Si AND Ag/Si WAFERS

*[1] Frantsevich Institute for Problems of Material Sciences of National Academy of Sciences of Ukraine*
*3 Krzhizhanovsky Str., Kyiv, 03142, Ukraine, E-mail: v_karpina@ukr.net*
*[2] V. Lashkaryov Institute of Semiconductor Physics of National Academy of Sciences of Ukraine*
*41 Nauki Ave., Kyiv, 03028, Ukraine*
*[3] D.K. Zabolotny Institute of Microbiology and Virology of National Academy of Sciences of Ukraine*
*154 Zabolotny Str., Kyiv, 03143, Ukraine*

*Zinc oxide nanostructures (NS) were grown on thin discontinuous films of noble metals of silver and gold in order to study their structure, optical properties as well as photocatalytic and antiviral activity. The paper presents the results of X-ray diffraction study, scanning electron microscopy study, photoluminescence and Raman measurements. X-ray diffraction experiments demonstrate similar patterns for all grown ZnO nanostructures. The SEM images of ZnO NS grown on Ag/Si and Au/Si wafers demonstrate more dense surface microstructure compared to ZnO NS grown on bare Si wafers. The most intensive ultraviolet and deep level emissions are observed for ZnO NS grown on Ag/Si wafers. Increase in thicknesses of Ag island film from 5 nm to 10 nm gives significant increase in intensity of ultraviolet and deep level emissions. Photocatalysis of grown ZnO nanostructures was studied by methyl orange dye degradation. Superior photocatalytic results are demonstrated by ZnO nanostructures grown on Ag/Si wafers, for which constants of dye degradation were twice higher than for ZnO nanostructures grown on Si and Au/Si substrates. The photocatalytic results correlates with photoluminescence spectra: more intensive photoluminescence in ultraviolet and visible ranges of optical spectrum leads to better photocatalytic performance. The cytotoxic effect of ZnO nanostructures was studied without photoactivation by the help of cell cultures MDCK and Hep-2 while the virucidal effect of ZnO nanostructures was studied by the help of Influenza A virus (H1N1) (strain FM / 1/47) and human adenovirus serotype 2 (HAdV2). ZnO nanostructures in a 1:10 dilution were not toxic to Hep-2 and MDCK cells. Most of the tested ZnO nanostructures exhibited no virucidal activity against human adenovirus serotype 2 (HAdV2) and influenza A virus (H1N1) (strain FM / 1/47) in the absence of photoexcitation.*

***Keywords**: ZnO, nanostructures, photoluminescence, Raman scattering, photocatalysis, cytotoxicity, virucidal activity*

## INTRODUCTION

Semiconductor photocatalysis is one of the promising processes used for the complete mineralization of a wide range of organic toxic chemicals. The wide-bandgap semiconductor material ZnO, like $TiO_2$, is considered as a good one for photocatalytic decomposition of hazardous materials such as dyes and organic compounds from waste water. ZnO in the form of various nanostructures (NS) is very promising photocatalysts because of increased surface area with high redox potential, high quantum efficiency, a good physical and chemical stability [1, 2]. In addition, it is non-toxic and low-cost material, suitable for large-scale production. ZnO photocatalysis can be improved by introduction various impurities in cationic or anionic sublattices [2]. One can expect improving photocatalytic activity of ZnO by dopand elements due to possibility to enhance the dye adsorption on the catalyst surface, to enhance UV absorption, to eliminate the electron-hole recombination and increase the number of charge carriers. Another brilliant idea directed to improve photocatalytic activity is to develop plasmonic-based materials in form of composite nanostructures such as metal/semiconductor, metal/insulator/semiconductor, and metal/semiconductor/semiconductor [3]. Plasmonic nanostructures are characterized by their strong

light absorption efficiency and photothermal effect both can boost overall kinetics of photochemical reactions. For example, being combined with Ag metal nanoparticles, photocatalysis and antimicrobial activity of ZnO can be greatly increased [4, 5] and cost effective antimicrobial surfaces can be developed. Indeed, photocatalytic materials not only effective for water and air purification from organic dye compounds but also can be used as antimicrobial coatings for pharmaceutical and food industries. The development of new photocatalytic materials with effective antimicrobial action is an important area of modern materials science. Many efforts have been devoted to inactivation of waterborne viruses and bacteria with photocatalytic materials [6].

With the increasing use of ZnO nanoparticles in cosmetic, biomedical, and industrial sectors, public awareness and concern have been raised about the safety of these nanomaterials. *In vitro* cell cultivation experiments demonstrate that ZnO exhibit adverse impacts and toxic effects to a number of mammalian cell lines, including human erythrocyte, human dermal fibroblast, human lymphocyte, *etc.* [7]. Accordingly, the cytotoxicity of ZnO NS should be carefully investigated.

In this work we investigate the influence of covering Si wafers with thin films of Au and Ag thin films on the structure, morphology, photocatalytic and antiviral activity of ZnO NS grown by atmospheric pressure metal-organic CVD (MOCVD) process. Earlier in [8], we successfully applied MOCVD method to growth well-defined Ag-doped ZnO nanocrystals and nanowires.

## EXPERIMENTAL DETAILS

Zinc oxide nanostructures were grown on Si wafers covered by thin films of noble metals (silver or gold) under the same conditions by MOCVD process at atmospheric pressure. The MOCVD process was realized in quartz tube arranged in horizontal tube furnace. Thin discontinuous films of Ag and Au with the mass thicknesses in the range 2–10 nm were deposited on (100) Si wafers by thermal evaporation process in vacuum chamber. At such small thicknesses, the metal films are discontinuous after deposition. As a result of being in the high-temperature zone, as in the MOCVD reactor, an island film morphology is formed [9]. In order to prevent the formation of metal and silicon alloys due to diffusion at high temperatures, a layer of $SiO_2$ with a thickness of ~5 nm was grown on Si wafers by thermal oxidation. Prepared Si, Ag/Si and Au/Si substrates were located in a zone with temperature of 500 °C. Zinc acetylacetonate precursor was loaded in a ceramic boat in amount of one gram. The boat was arranged in the quartz tube at a position where temperature was settled to 300 °C. The one end of the quartz tube was tightly closed while the other was open. Time of ZnO NS growth was 30 min. Substrates with ZnO NS grown were left in cooled furnace by 1 h before extraction.

The structure of grown ZnO nanostructures was characterized by X-ray diffraction (XRD) measurements carried out on a DRON-3 diffractometer in Bragg-Brentano configuration using Cu$K_\alpha$ radiation ($\lambda = 0.1542$ nm). Scanning electron microscope (SEM) Tescan Mira 3 LMU was used to surface morphology characterization. Photoluminescence (PL) of deposited films were excited using a He-Cd laser with the photon energy $h\nu = 3.81$ eV (325 nm). The Raman measurements were carried out in a quasi-back scattering geometry at room temperature using a Horiba Jobin-Yvon T64000 triple spectrometer with an integrated micro-Raman setup – Olympus BX-41 microscope equipped with a Peltier-cooled CCD detector. The experiments were carried out using the 488 nm line of an Ar/Kr laser.

Photocatalysis of ZnO NS was studied by decomposition of methyl-orange (MO) dye with initial concentration $C_0 = 10$ mg/l upon Hg lamp irradiation with power of 200 W during 3–12 h. No optical filters were used. The size of all samples for photocatalysis experiments was 1×1 cm$^2$. Before illumination, the investigated samples placed in MO aqueous solution were kept in the dark during 30 min to achieve an adsorption–desorption equilibrium. The residual concentration of dye, $C$, was calculated from minima of MO transmission spectra at wavelength 465 nm. The photocatalytic efficacy of dye decomposition can be expressed as changing $C/C_0$ ratio with a time in accordance with pseudo-first order model for low dye concentrations: $\ln (C/C_0) = K^*t$, where $C_0$ and $C$ are the concentrations of dye in the aqueous solution at time $t = 0$ and certain time $t$ respectively, and $K$ is the pseudo-first order rate [10].

Cell cultures used in experiments were MDCK (Madin-Darby Canine Kidney cells) and Hep-2 (Larynx Epidermoid Carcinoma) in accordance with [11]. The Influenza A virus (H1N1) (strain FM/1/47) and human adenovirus serotype 2 (HAdV2) were obtained from the collection of the Institute of Epidemiology and Infectious Diseases of the Academy of Medical Sciences of Ukraine and the Institute of Microbiology, Medical University of Budapest (Hungary), respectively.

To study the cytotoxic effect a susbstrate with ZnO nanostructures were placed in the wells of a 24-well plate with 1 ml of DMEM medium (Biowest, France). The plate was kept at 37 °C in an atmosphere of 5 % $CO_2$ for 24 h. The washes were selected and a series of ten-fold dilutions were prepared. Cell cultures in a 96 well plate after 1 day of growth and formation of 70–90 % of the monolayer were washed from the culture medium. Diluted washes were added at 100 µl/well in triplicate. Wells with DMEM medium were used as a cell control. The plates were kept for 72 h at 37 °C in an atmosphere of 5 % $CO_2$. Cell viability was studied using MTT solution (Sigma, USA) according to standard methods [12].

To study the virucidal effect, a susbstrate with ZnO nanostructures were placed in the wells of a 24-well plate, and 50 µl of undiluted virus-containing material was applied to the surface of nanomaterial. A square of Parafilm M (Bemis, USA) with an area of 1 $cm^2$ was covered on top to prevent drying of the material and better contact of the virus with the surface of the nanostructure. The plate was kept for 1 h in the dark environment at room temperature and 450 µl/well of support medium was added. The virus was suspended and selected for study, preparing a series of 10-fold dilutions. Further study of the virucidal effect of nanostructures was carried out according to the classical method. Cells were cultured for 72 h until a pronounced cytopathogenic effect (CPE) was formed in the control of the virus. A decrease in the infectious titer of the virus by 5–2 lg $TCID_{50}$ /ml ($TCID_{50}$ /ml is the median tissue culture infectious dose) and more, compared with the control of the virus, indicates a virucidal effect [13].

## STRUCTURE AND OPTICAL PROPERTIES

Fig. 1 presents X-ray diffraction patterns of the grown ZnO, ZnO/Au and ZnO/Ag nanostructures on the (100) Si substrates. Besides reflexes of monocrystal Si substrate, the presented XRD patterns include the intense reflexes at 2θ angles 31.77, 34.42 and 36.25°, which correspond to the reflection of X-rays from the (100), (002) and (101) planes of the hexagonal wurtzite structure of zinc oxide. No peaks caused by the presence of other components were detected. For ZnO/Ag and ZnO/Au nanostructures, the XRD patterns are almost identical which indicates a weak influence of the nature of the thin metal film on the nucleation and growth of ZnO nanostructures.

Fig. 2 presents SEM images of ZnO nanostructures grown on the surface of cleaned factory polished Si as well as Si with ultrathin discontinuous Au or Ag films. Basically, ZnO NS demonstrate developed surface morphology with agglomerated ZnO microparticles. Each agglomeration itself consists of spherical ZnO microparticles the surface of which, in turn, covered by nanograins having size in range 17–24 nm. It can be seen that there are also uncovered places on Si wafer. Thus, such morphology provides contact of dye not only with ZnO nanoparticles but also with Si wafer covered by thin films of noble metals that is important for photocatalysis. ZnO NS grown on Ag/Si and Au/Si wafers demonstrate more dense surface microstructure compared to ZnO NS grown on bare Si wafers.

Fig. 3 shows room-temperature PL spectra of ZnO, ZnO/Ag, ZnO/Au NS. PL spectra consist of two energetically separated bands: one is ultraviolet band arount 380 nm, the other – a wide visible band in the range 470–600 nm. The ultraviolet band is a near-band edge emission (NBE) of ZnO due to the radiative recombination of free excitons [14]. The broad band in visible part of the optical spectrum is a deep-level emission (DLE) which corresponds to optical radiative transition between conduction or valence band and various energy levels in forbidden band appeared as a result intrinsic point defects, namely, oxygen vacancy ($V_O$) in various charge state, oxygen interstitials ($O_i$), oxygen antisite ($Zn_O$), zinc vacancy ($V_{Zn}$), zinc interstitials ($Zn_i$) and zinc antisite ($O_{Zn}$) [15]. Among these intrinsic defects the oxygen vacancies in ZnO nanostructures in various charge states are considered to be greatly influence on processes of electron-hole recombination and thus on efficiency of photocatalysis.

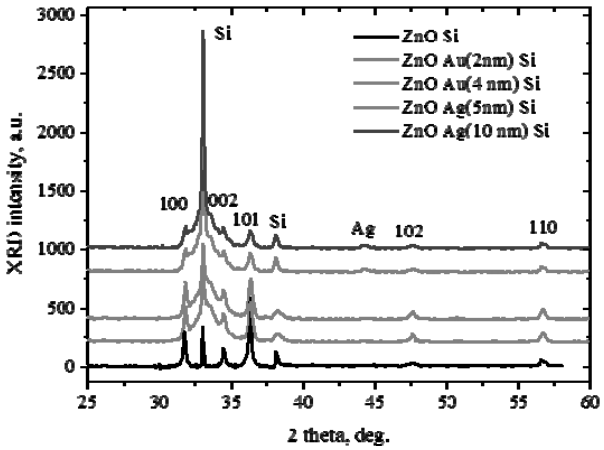


**Fig. 1.** XRD patterns of ZnO, ZnO/Au and ZnO/Ag NS grown on Si by MOCVD

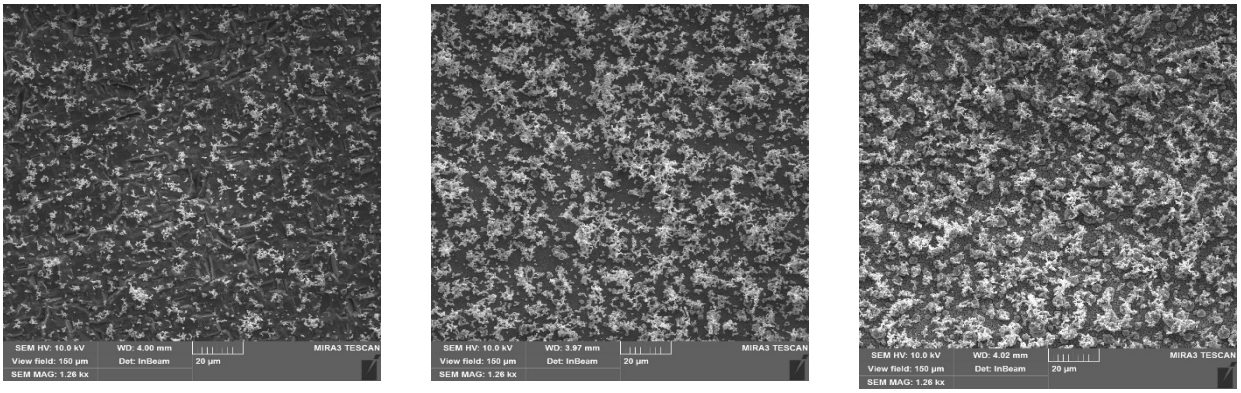

ZnO/Si
*a*

ZnO/Au(2 nm)/Si
*b*

ZnO/Ag (5 nm) /Si
*c*

**Fig. 2.** SEM images of surface morphology of ZnO nanostructures grown on bare Si (*a*) as well as on Si covered with discontinuous Au (*b*) and Ag (*c*) films

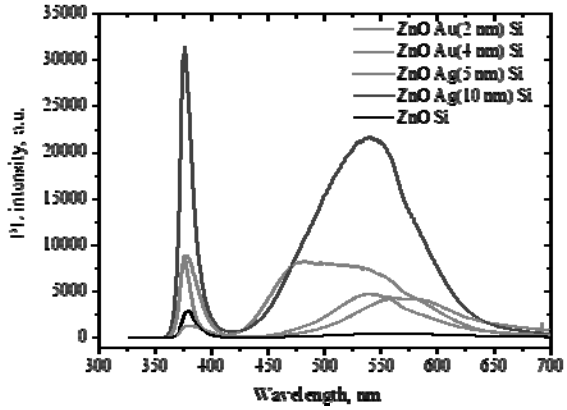


**Fig. 3.** Room-temperature photoluminescence spectra of ZnO, ZnO/Ag and ZnO/Au NS. $\lambda_{exc}$ = 325 nm

As one can see from Fig. 3, DLE emission is very low for ZnO NS grown on bare Si wafers compared to ZnO NS grown on Ag/Si and Au/Si wafers. This is a result of a good crystal quality of grown ZnO NS on bare Si wafers. On the contrary, ZnO NS grown on Au/Si wafers demonstrate both intense NBE emission and DLE emission with two peaks around 540 nm and 580 nm, correlated with $V_O$ and $O_i$ defects correspondingly [16]. The most intensive UV and DLE emissions are observed for ZnO NS grown on Ag/Si wafers. Increase in thicknesses of Ag island film from 5 to 10 nm gives significant increase in intensity of UV and DLE emissions. Moreover, ZnO/Ag/Si NS demonstrate a distinct PL peak at 475 nm which is not observed in ZnO/Au/Si and ZnO/Si NS. This peak is attributed to Ag metal impurity. One possible explanation is formation of deep acceptor level $Ag_{Zn}$ as a result of silver diffusion into the zinc oxide lattice. In this case the optical transitions between shallow $Zn_i$ donor levels and deep acceptor level $Ag_{Zn}$ are possible [17]. Another explanation is enhancing of PL emission at 475 nm as a result of influence island silver film due to surface plasmon resonance as it was previously reported in [17]. Moreover, PL enhancement in ultraviolet-blue region was also observed in [18, 19] for ZnO NS coated with noble island metal films. We have also observed in [8] that increase in Ag dopant content for Ag-doped ZnO NS as well as increase in growth temperature range leads to significant increase in the intensity of DLE and NBE emission bands. Thus, ZnO NS grown on Ag/Si wafers exhibit enhanced PL that can be a result of plasmonic enhancement or Ag impurity ions diffusion indicating on a possible enhanced photocatalytic performance.

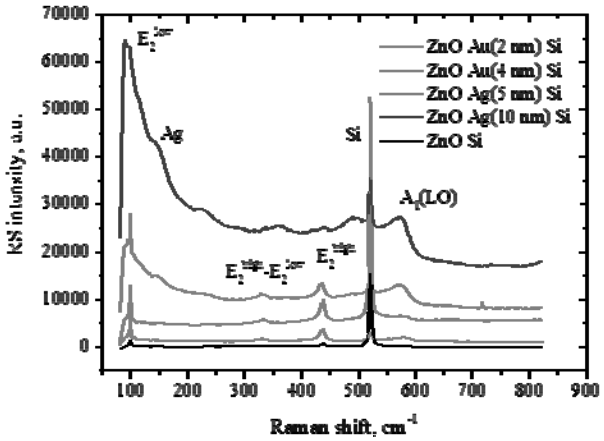


**Fig. 4.** Raman spectra of ZnO NS grown on Si, Ag/Si and Au/Si substrates

The method of Raman scattering was used to study the effect of thin island Ag and Au films on the crystal quality and vibrational properties of grown ZnO NS. The studies were performed in the configuration where only $E_2^{low}$, $E_2^{high}$ and $A_1$(LO) modes are allowed for the ZnO wurtzite structure according to the symmetry selection rules [20]. Fig. 4 shows the Raman spectra of ZnO NS as well as ZnO/Ag and ZnO/Au NS. Intensive $E_2^{low}$ phonon mode at 98 $cm^{-1}$, $E_2^{high}$ phonon mode at 437 $cm^{-1}$ and $qA(E)_1$(LO) are observed in Raman spectra for all grown ZnO NS. The $E_2^{high}$ mode is associated exclusively with oxygen sublattice oscillations, and the $E_2^{low}$ phonon mode is caused by oscillations in zinc sublattice [21]. The band at 574 $cm^{-1}$ is attributed to $A_1$(LO) phonon mode. This mode is caused by the disorder of the crystal structure, in particular, the presence of such point defects as oxygen vacancies, zinc interstitials or their complexes. It is pronounced for ZnO/Ag NS. Other weak band is located at 334 $cm^{-1}$ which is believed to be second-order Raman scattering that arose from zone-boundary (M point) phonons $E_2^{high}$-$E_2^{low}$(M). One can observe a significant change in the shape and intensity of $E_2^{low}$, $E_2^{high}$ and $A_1$(LO) phonon modes for ZnO NS grown on Ag/Si wafers caused by the presence of a silver film on a silicon wafer. This indicates on an increase of disordering in crystal structure of ZnO/Ag NS compared to ZnO and ZnO/Au NS. Moreover, at the right hand of $E_2^{low}$

phonon mode the intensive wide band at 146 $cm^{-1}$ is appeared for ZnO/Ag NS. The intensity of this band increases with the thickness of Ag film. We believed that this band can be attributed to vibrational mode of Ag lattice [22].

## PHOTOCATALYSIS AND ANTIVIRAL ACTIVITY

Photocatalytic destruction of MO dye was studied under irradiation of samples with full spectrum of Hg lamp. Every three hours of irradiation the transmission spectra of MO dye were recorded and residual concentrations of dye were calculated. The obtained results of photocatalytic destruction of MO dye are presented in Fig. 5. The degradation rate constant $K$ calculated from the first-order model $\ln(C/C_0) = K \cdot t$-for grown ZnO nanostructures are presented in Fig. 5 also. Self-degradation of MO dye did not exceed 10 %. As can be seen from Fig. 5, the best results demonstrate ZnO nanostructures grown on Ag/Si wafers. For these nanostructures constant of dye degradation $K$ was twice larger than ones for ZnO/Si and ZnO/Au/Si samples. This enhanced value can be obliged to Ag coating, that can provide more effective charge transfer from ZnO semiconductor to dye molecules [23]. ZnO/Au/Si samples with Au thin films of different thicknesses did not provide better photocatalytic activity than ZnO/Si samples. Here, we can suppose that better photocatalytic properties of ZnO/Ag/Si samples can be related to excitation of localized surface plasmons in Ag nanoparticle films or Ag diffusions into ZnO NS at their growth. The energy of surface plasmons in silver nanoparticles is close to band gap energy of ZnO that can provide more efficient way to charge transfer or PL enhancement. The kinetics of photocatalysis also correlates with PL measurements. Strong PL in UV range together with strong emission in visible part of optical spectrum provides better photocatalysis.

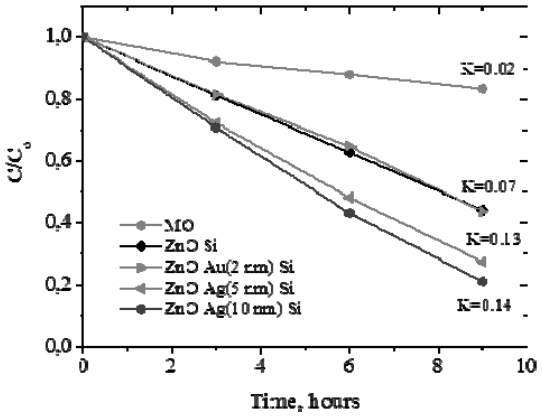


**Fig. 5.** Kinetics of MO dye photodegradation by the help of ZnO, ZnO/Ag and ZnO/Au NS deposited on Si wafers under illumination with 200 W Hg lamp

Cytotoxic effect of ZnO NS grown on Au/Si and Ag/Si wafers against Hep-2 cells in various dilutions was studied during 24–72 h. The results presented in Fig. 6 demonstrate that in dilutions 1:1 and 1:10 the fraction of alive Hep-2 cells was about 20 %. In dilutions 1:100 ZnO NS were non-toxic against Hep-2 cells. Fig. 7 demonstrates cytotoxic effect of ZnO NS grown on Au/Si and Ag/Si wafers against MDCK cells. We can conclude that investigated ZnO nanostructures were slightly toxic to MDCK cells, and even in a 1:10 dilution, they did not inhibit cell proliferation. So, washes of ZnO NS for Hep-2 cells and MDCK cells in undiluted solutions were all toxic. Diluted washes lead to losing of their cytotoxic effect.

Most of the tested ZnO NS did not exhibit virucidal activity against human adenovirus serotype 2 (HAdV2) and influenza A virus (H1N1) strain A/FM/1/47, as evidenced by a slight decrease or increase in virus titer in the presence of nanostructures (see Table). Lack of suppression of virus reproduction can be explained by the fact that all experiments were carried out in the dark without light irradiation and, hence, without photocatalytic reactions.

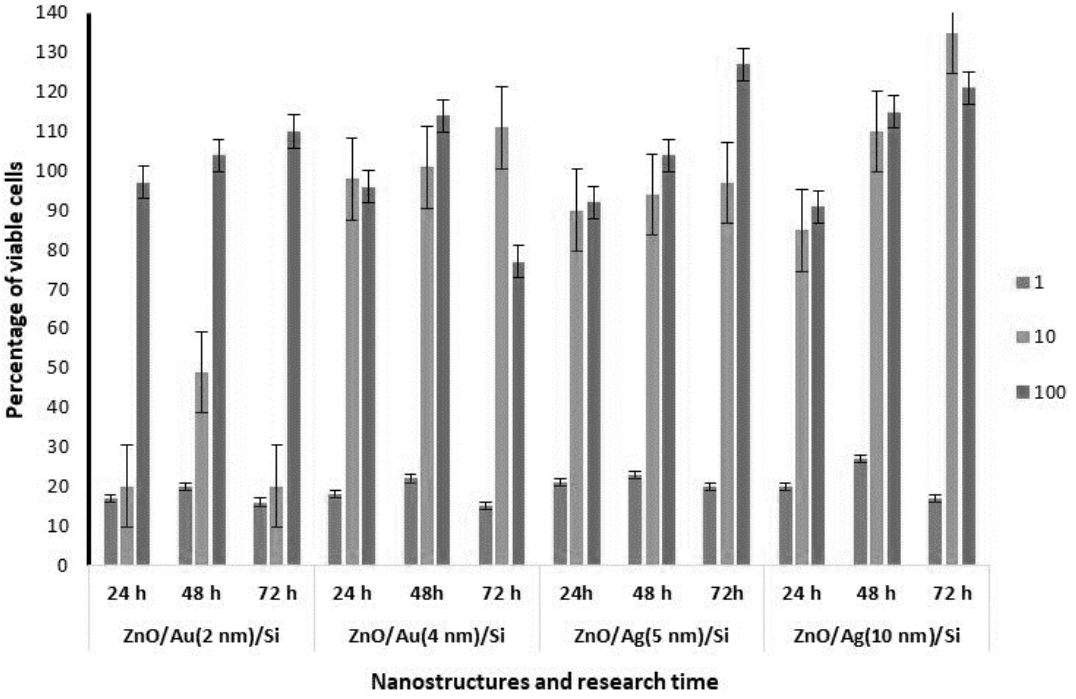


**Fig. 6.** Cytotoxic effect of zinc oxide nanostructures grown on Au/Si and Ag/Si substrates against Hep-2 cells in various dilutions during 24-72 hours

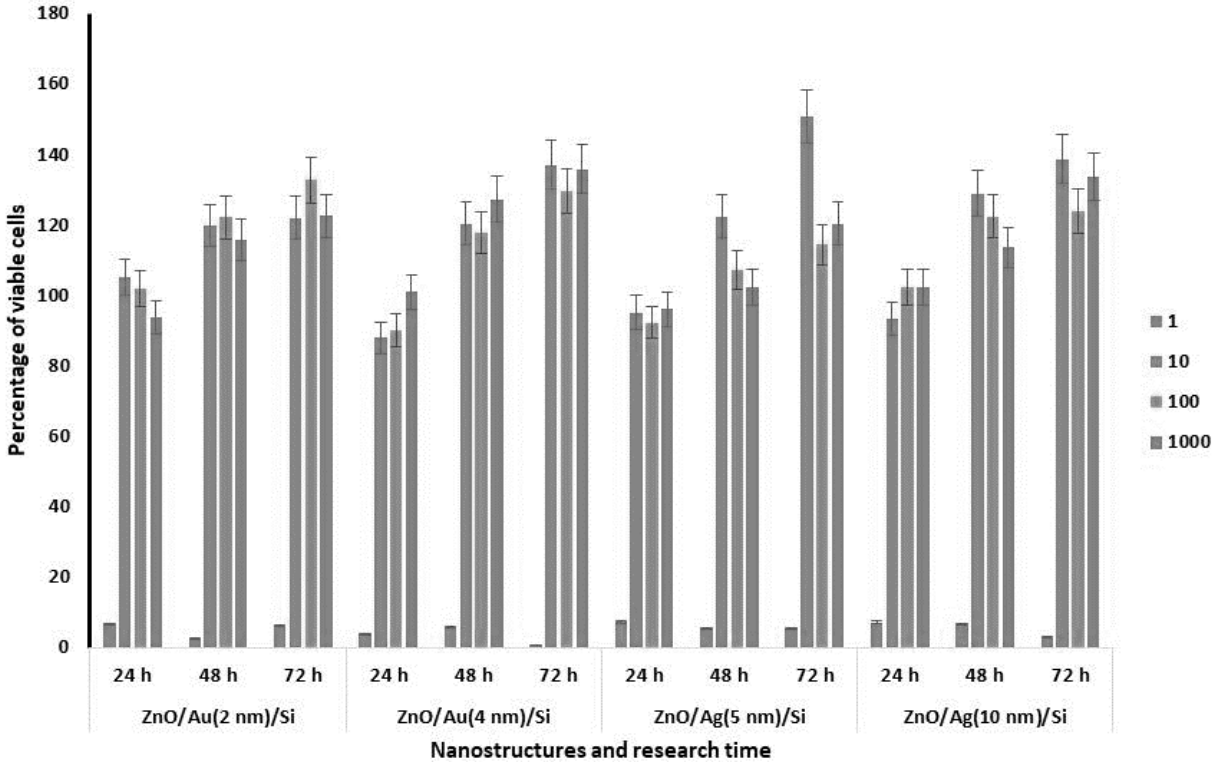


**Fig. 7.** Cytotoxic effect of zinc oxide nanostructures grown on Au/Si and Ag/Si substrates against MDCK cells in various dilutions during 24-72 hours

**Table.** Adenovirus serotype 2 (HAdV2) and H1N1 virus titers in the presence of ZnO NS grown on Au/Si and Ag/Si substrates

| Sample | Titer, lg $TCID_{50}$/ml | Titer difference |
|---|---|---|
| HAdV2 (control) | 5.75 | |
| HAdV2 + ZnO/ Au (2 nm)/Si | 6.32 | +0.57 |
| HAdV2+ ZnO/ Au (4 nm)/Si | 6.49 | +0.74 |
| HAdV2+ ZnO/ Ag(5 nm)/Si | 6.52 | +0.77 |
| HAdV2+ ZnO/ Ag(10 nm)/Si | 6.08 | +0.13 |
| H1N1 (control) | 6.98 | |
| H1N1 + ZnO/ Au (2 nm)/Si | 6.13 | -0.85 |
| H1N1+ ZnO/ Au (4 nm)/Si | 7.13 | +0.15 |
| H1N1+ ZnO/ Ag(5 nm)/Si | 6.44 | -0.54 |
| H1N1+ ZnO/ Ag(10 nm)/Si | 6.70 | -0.28 |

## CONCLUSIONS

Zinc oxide nanostructures were grown by MOCVD on thin discontinuous films of noble metals of silver and gold on Si wafers in order to study their photocatalytic and virucidal activity. SEM and XRD measurements have shown that nanostructures fabricated demonstrate developed surface morphology with agglomerated near-spherical ZnO micro- and nanoparticles with size down to 17–24 nm. Morphology of ZnO nanoparticle aggregates grown on Si, Au/Si and Ag/Si wafers practically identical. But Raman measurements demonstrate significant difference between ZnO/Ag/Si and ZnO/Au/Si NS. Increased intensity of $A_1LO$ phonon mode for ZnO/Ag/Si NS compared to ZnO/Si and ZnO/Au/Si NS indicates on an increase of disordering in ZnO crystal structure at presence of Ag. However, photocatalytic activity of ZnO/Ag/Si samples is two times higher than ones for ZnO/Au/Si and ZnO/Si samples. It is also shown that photoluminescence of ZnO NS grown on Ag/Si wafers were enhanced in UV and visible ranges of optical spectrum. Thus, the presence of a thin Ag film on Si wafer provide more efficient way to charge transfer from semiconductor ZnO to MO dye molecules that is obliged to ZnO PL enhancement due to excitation of surface plasmons in metal film or silver diffusion into ZnO nanoparticles at their growth. ZnO NS in a 1:10 dilution were not toxic to Hep-2 and MDCK cells. Without photoactivation tested ZnO NS did not exhibit virucidal activity against human adenovirus serotype 2 (HAdV2) and influenza A virus (H1N1) strain A/FM/1/47, as evidenced by a slight decrease or increase in virus titer in the presence of nanostructures. In the future, it is worth while to investigate the effect of nanostructures on the infectious titers of viruses at photoactivation.

## ACKNOWLEDGEMENTS

This work was partially supported by the research projects of NAS of Ukraine “The development of photocatalytic nanocomposites for viruses inactivation in the air”.

# Фотокаталіз та оптичні властивості наноструктур ZnO, вирощених на пластинах Si, Au/Si та Ag/Si методом MOCVD

**В.А. Карпина, Л.А. Миронюк, Д.В. Миронюк, М.Е. Бугайова, Л.І. Петросян, О.І. Биков, О.І. Оліфан, В.В. Стрельчук, О.Ф. Коломис, В.Р. Романюк, К.С. Науменко, Л.О. Артюх, О.Ю. Повниця, С.Д. Загородня, А.І. Євтушенко**

*Інститут проблем матеріалознавства ім І.М. Францевича Національної академії наук України*
*вул. Академіка Кржижановського, 3, Київ, 03142, Україна, v_karpina@ukr.net*
*Інститут фізики напівпровідників ім. В.Є. Лашкарьова Національної академії наук України*
*пр. Науки, 41, Київ, 03028, Україна*
*Інститут мікробіології і вірусології ім. Д.К. Заболотного Національної академії наук України*
*вул. Академіка Заболотного, 154, Київ, 03143, Україна*

*Наноструктури (НС) оксиду цинку вирощено на тонких острівцевих плівках благородних металів срібла та золота з метою вивчення їхньої фотокаталітичної активності. Рентгенограми показують, що НС на поверхні Si, Au/Si та Ag/Si підкладках не є текстурованими і складаються із кристалітів з різною орієнтацією. Зображення СЕМ свідчать про те, що наноструктури ZnO демонструють розвинену 3D морфологію з агломерованими мікрочастинками ZnO. Методами рентгенівського дифракційного аналізу та СЕМ встановили, що мікроструктура вирощених на пластинах Si, Au/Si та Ag/Si наноструктур ZnO практично ідентична, але вимірювання комбінаційного розсіювання світла демонструють значну різницю між НС ZnO/Ag/Si та НС ZnO/Au/Si. Збільшення інтенсивності фононної моди A1(LO) для НС ZnO/Ag/Si порівняно з НС ZnO/Si та ZnO/Au/Si свідчить про збільшення розупорядкованості кристалічної структури. Виявлено, що фотокаталітична активність зразків ZnO/Ag/Si вдвічі вища, ніж для зразків ZnO/Au/Si та ZnO/Si. Показано, що фотолюмінесценція НС ZnO, вирощених на пластинах Ag/Si, була підсиленою як в УФ, так і у видимому діапазонах оптичного спектра. Таким чином, наявність тонкої плівки Ag на підкладці Si забезпечує більш ефективний спосіб перенесення заряду від напівпровідника ZnO до молекул барвника МО, що може бути зумовлено збудженням поверхневих плазмонних коливань у острівцевій металевій плівці або дифузією срібла в НС ZnO. Встановлено, що НС ZnO у розведенні 1:10 не були токсичними для клітин Hep-2 та MDCK. Досліджувані НС ZnO без фотоактивації не проявляли віруліцидної активності проти аденовірусу людини серотипу 2 (HAdV2) і вірусу грипу А (H1N1) штаму A/FM/1/47, про що свідчить невелике зниження або підвищення титру вірусу в присутності наноструктур. У майбутньому перспективним є дослідити вплив наноструктур ZnO на інфекційні титри вірусів при фотоактивації.*

***Ключові слова**: ZnO, наноструктури, фотолюмінесценція, комбінаційне розсіювання, фотокаталіз, цитотоксичність, віруліцидна активність*

REFERENCES

1. Baibara O.E., Radchenko M.V., Karpyna V.A., Ievtushenko A.I. A review of the some aspects for the development of ZnO based photocatalysts for a variety of applications. *Phys. Chem. Solid State.* 2021. **22**(3): 585.
2. Qi K., Cheng B., Yu J., Ho W. Review on the improvement of the photocatalytic and antibacterial activities of ZnO. *J. Alloys Compd.* 2017. **727**: 792.
3. Wang D., Pillai S.C., Ho S.-H., Zeng J., Li Y., Dionysiou D.D. Plasmonic-based nanomaterials for environmental remediation. *Appl. Catal. B.* 2018. **237**: 721.
4. Xie W., Li Y., Sun W., Huang J., Xie H., Zhao X. Surface modification of ZnO with Ag improves its photocatalytic efficiency and photostability. *J. Photochem. Photobiol. A.* 2010. **216**(2–3): 149.
5. Bouzid H., Faisal M., Harraz F.A., Al-Sayari S.A., Ismail A.A. Synthesis of mesoporous Ag/ZnO nanocrystals with enhanced photocatalytic activity. *Catal. Today.* 2015. **252**: 20.
6. Zhang C., Li Y., Shuai D., Shen Y., Wang D. Progress and challenges in photocatalytic disinfection of waterborneViruses: A review to fill current knowledge gaps. *Chem. Eng. J.* 2019. **355**: 399.
7. Liao C., Jin Y., Li Y., Tjong S.C. Interactions of Zinc Oxide Nanostructures with Mammalian Cells: Cytotoxicity and Photocatalytic Toxicity. *Int. J. Mol. Sci.* 2020. **21**(17): 6305.

8. Ievtushenko A., Karpyna V., Eriksson J., Tsiaoussis I., Shtepliuk I., Lashkarev G., Yakimova R., Khranovskyy V. Effect of Ag doping on the structural, electrical and optical properties of ZnO grown by MOCVD at different substrate temperatures. *Superlattices Microstruct*. 2018. **117**: 121.
9. Romanyuk V.R., Kondratenko O.S., Kondratenko S.V., Kotko A.V., Dmitruk N.L. Transformation of thin gold films morphology and tuning of surface plasmon resonance by post-growth thermal processing. *Eur. Phys. J. Appl. Phys*. 2011. **56**(1): 10302.
10. Ahmad M., Ahmed E., Zhang Y., Khalid N.R., Xu J., Ullah M., Hong Z. Preparation of highly efficient Al-doped ZnO photocatalyst by combustion synthesis. *Curr. Appl. Phys.* 2013. **13**(4): 697.
11. European Collection of Animal Cell Cultures Catalog. Porton Down: Salisbury (UK) PHLS Centre of Applied Microbiology and Research, 1990.
12. He Y.T., Wan J., Tokunaga T. Kinetic stability of hematite nanoparticles: the effect of particle sizes. *J. Nanopart. Res.* 2008. **10**: 321.
13. Kohn L.K., Foglio M.A., Rodrigues R.A., Sousa I.M., Martini M.C., Padilla M.A. In-Vitro Antiviral Activities of Extracts of Plants of The Brazilian Cerrado against the Avian Metapneumovirus (aMPV). *Rev. Bras. Cienc. Avic.* 2015. **17**(3): 275.
14. Zhang Y., Lin B., Sun X., Fu Z. Temperature-dependent photoluminescence of nanocrystalline ZnO thin films grown on Si (100) substrates by the sol-gel process. *Appl. Phys. Lett.* 2005. **86**(13): 131910.
15. Galdámez-Martinez A., Santana G., Güell F., Martínez-Alanis P.R., Dutt A. Photoluminescence of ZnO Nanowires: A Review. *Nanomaterials.* 2020. **10**(5): 857.
16. Karpyna V., Ievtushenko A., Kolomys O., Lytvyn O., Strelchuk V., Tkach V., Starik S., Baturin V., Karpenko O. Raman and Photoluminescence Study of Al,N-Codoped ZnO Films Deposited at Oxygen-Rich Conditions by Magnetron Sputtering. *Phys. Status Solidi B.* 2020. **257**(6): 1900788.
17. Ko Y.H., Yu J.S. Silver nanoparticle decorated ZnO nanorod arrays on AZO films for light absorption enhancement. *Phys. Status Solidi A.* 2012. **209**(2): 297.
18. Singh T., Pandya D.K., Singh R. Surface plasmon enhanced bandgap emission of electrochemically grown ZnO nanorods using Au nanoparticles. *Thin Solid Films.* 2012. **520**(14): 4646.
19. Cheng P., Li D., Yuan Z., Chen P., Yang D. Enhancement of ZnO light emission via coupling with localized surface plasmon of Ag island film. *Appl. Phys. Lett.* 2008. **92**(4): 041119.
20. Damen T.C., Porto S.P.S., Tell B. Raman Effect in Zinc Oxide. *Phys. Rev*. 1966. **142**(2): 570.
21. Sharma S.K., Exarhos G.J. Raman Spectroscopic Investigation of ZnO and Doped ZnO Films, Nanoparticles and Bulk Material at Ambient and High Pressures. *Solid State Phenomena*. 1997. **55**: 2.
22. Strelchuk V.V., Kolomys O.F., Golichenko B.O., Boyko M.I., Kaganovich E.B., Krishchenko I.M., Kravchenko S.O., Lytvyn O.S., Manoilov E.G., Nasieka Iu.M. *Semicond. Phys. Quantum Electron. Optoelectron.* 2015. **18**(1): 46.
23. Kuriakose S., Choudhary V., Satpati B., Mohapatra S. Enhanced photocatalytic activity of Ag–ZnO hybrid plasmonic nanostructures prepared by a facile wet chemical method. *Beilstein J. Nanotechnol.* 2014. **5**: 639.


*Received 31.08.2022, accepted 03.03.2023*